

SPATIAL AND DYNAMICAL BIASES IN VELOCITY STATISTICS OF GALAXIES

KOJI YOSHIKAWA

Research Center for the Early Universe (RESCEU), School of Science, University of Tokyo, Tokyo 113-0033, Japan;
 kohji@utap.phys.s.u-tokyo.ac.jp

Y. P. JING

Shanghai Astronomical Observatory, Partner Group of MPI für Astrophysik, Nandan Road 80, Shanghai 200030, China;
 ypjing@center.shao.ac.cn

AND

GERHARD BÖRNER

Max-Planck-Institut für Astrophysik, Karl-Schwarzschild-Strasse 1, 85748 Garching, Germany;
 grb@mpa-garching.mpg.de

Received 2002 October 21; accepted 2003 February 28

ABSTRACT

We present velocity statistics of galaxies and their biases inferred from the statistics of the underlying dark matter using a cosmological hydrodynamic simulation of galaxy formation in low-density and spatially flat ($\Omega_0 = 0.3$ and $\lambda_0 = 0.7$) cold dark matter cosmogony. Our simulation is based on a particle-particle-particle-mesh (P³M) N -body Poisson solver and smoothed particle hydrodynamics. Galaxies in our simulation are identified as clumps of cold and dense gas particles and classified as young and old galaxies according to their formation epochs. We find that the pairwise velocity dispersion (PVD) of all galaxies is significantly lower than that of the dark matter particles and that the PVD of the young galaxies is lower than that of the old types, and even of all galaxies together, especially at small separations. These results are in reasonable agreement with the recent measurements of PVDs in the Las Campanas redshift survey, the *IRAS* Point Source Catalogue Redshift Survey, and the Sloan Digital Sky Survey data. We also find that the low PVD of young galaxies is due to the effects of dynamical friction as well as the different spatial distribution, while the difference in the PVD between all galaxies and dark matter can be mostly ascribed to their different spatial distributions. We also consider the mean infall velocity and the POTENT density reconstruction that are often used to measure the cosmological parameters, and investigate the effects of spatial bias and dynamical friction. In our simulation, the mean infall velocity of young galaxies is significantly lower than that of all the galaxies or of the old galaxies, and the dynamical bias becomes important on scales less than $3 h^{-1}$ Mpc. The mass density field reconstructed from the velocity field of young galaxies using the POTENT-style method suffers in accuracy from both the spatial bias and the dynamical friction on the smoothing scale of $R_s = 8 h^{-1}$ Mpc. On the other hand, in the case of $R_s = 12 h^{-1}$ Mpc, which is typically adopted in the actual POTENT analysis, the density reconstruction based on various tracers of galaxies is reasonably accurate. We also analyze the motions of central galaxies and the velocity dispersion of galaxies within halos and discuss their implications for the motion of cD galaxies and the determination of the mass of galaxy groups.

Subject headings: galaxies: clusters: general — large-scale structure of universe — methods: numerical

1. INTRODUCTION

There have been many attempts to model the dark matter distribution in the universe using the velocity information of galaxies, based on the assumption that the velocity is induced by the gravity. The peculiar velocity of galaxies can either be measured from secondary distance indicators (e.g., the Tully-Fisher relation for spiral galaxies and the fundamental plane for elliptical galaxies) or it can be inferred from the distortion of the galaxy distribution in redshift space. Two simple statistics are often used to describe the velocity of galaxies: the mean infall velocity $v_{12}(r)$ and the pairwise velocity dispersion $\sigma_{12}(r)$ (hereafter PVD). These statistics are extensively used to constrain the density parameter Ω_0 of the universe and the clustering of dark matter on small scales (Davis & Peebles 1983; Davis et al. 1985; Ostriker & Suto 1990; Mo, Jing, & Börner 1993; Fisher et al. 1994; Suto & Jing 1997; Jing, Mo, & Börner 1998; Juszkiewicz et al. 2000; Jing, Börner, & Suto 2002; Zehavi et al. 2002). In addition, the observed peculiar velocity of galaxies has been used to measure the density field of the

nearby universe and the parameter $\beta \equiv \Omega_0^{0.6}/b$ by a number of authors (Bertschinger & Dekel 1989; Dekel 1994; Nusser & Davis 1994; Sigad et al. 1998; Dekel et al. 1999; Peacock et al. 2001; Zaroubi 2002). Here b is the linear bias factor of galaxy clustering.

Using the Las Campanas Redshift Survey (LCRS) of galaxies (Shectman et al. 1996), Jing et al. (1998) analyzed the PVD of galaxies and measured $\sigma_{12} = 580 \pm 80$ km s⁻¹ at the projected separation $r_p = 1 h^{-1}$ Mpc. The uncertainty quoted was obtained from an analysis of a set of mock samples. Since the LCRS contains about a few tens of clusters of galaxies, the PVD can be determined from this survey to an accuracy of 15% (including the cosmic variance). The result has been recently confirmed by Zehavi et al. (2002) and Hawkins et al. (2003), who measured the PVD of galaxies for the Early Data Release of the Sloan Digital Sky Survey (SDSS) and the Two-Degree Field Galaxy Redshift Survey (2dFGRS), respectively. In addition, it has been found that the PVD of late-type galaxies is smaller than that of early-type ones (Mo, Jing, & Börner 1993; Fisher et al. 1994). Jing et al. (2002) extensively analyzed the PVD of the galaxies in

the *IRAS* Point Source Catalogue Redshift Survey (PSCz; Saunders et al. 2000), which are mostly late-type galaxies, and found that the PVD is about $\sim 400 \text{ km s}^{-1}$ at $r_p = 2 h^{-1} \text{ Mpc}$ and rapidly decreases to $\sim 200 \text{ km s}^{-1}$ at small separation $r_p = 0.2 h^{-1} \text{ Mpc}$. This finding for the *IRAS* galaxies is again in good agreement with the SDSS result for blue or late-type galaxies by Zehavi et al. (2002). As for the PVD of dark matter, a number of previous numerical works (e.g., Benson et al. 2000; Suto 1993; Jenkins et al. 1998; Jing et al. 1998, 2002) conclude that the PVD of dark matter is $\sigma_{12} \simeq 700\text{--}800 \text{ km s}^{-1}$ at $r_p = 1 h^{-1} \text{ Mpc}$ for the spatially flat low-density cold dark matter universe and systematically higher than those of observed galaxies.

There are two causes for the difference between the velocity dispersion of galaxies and of dark matter. One is the fact that galaxies are distributed spatially differently from dark matter particles. Indeed, Jing et al. (1998) proposed a cluster (under-) weighted (CLW) model to explain both the spatial two-point correlation function and the pairwise velocity dispersion measured in the LCRS in popular flat low-density cold dark matter (LCDM) models. In this model, it is assumed that the number of galaxies per unit mass is a decreasing function of the hosting cluster (halo) mass; i.e., galaxies are antibiased in rich cluster regions (see Carlberg et al. 1996 and Bahcall & Comerford 2002 for the observational evidence for the antibiasing). The resulting difference in the PVDs between galaxies and dark matter is purely due to the difference between the two populations in their spatial distribution. We call this bias in the velocity statistics the “spatial bias.” Assuming that the *IRAS* galaxies are more strongly antibiased in rich cluster regions than the optical galaxies, Jing et al. (2002) found that the spatial clustering and the PVD of *IRAS* galaxies can be quantitatively explained in the popular LCDM models, except for the rapid decrease of the PVD at small separations observed for the *IRAS* galaxies.

Another cause for the velocity bias is dynamical friction. Because of this mechanism, the motion of galaxies could be systematically slower than that of dark matter particles within a host halo. We call this bias the “dynamical bias.” There have been many studies to quantify dynamical biases, but no consensus has been reached regarding to what extent the velocity statistics are affected by the dynamical bias (Katz, Hernquist, & Weinberg 1992; Frenk et al. 1996; Cen & Ostriker 2000; Pearce et al. 2001). In Jing et al. (2002), it was conjectured that the rapid decrease of the PVD of *IRAS* galaxies is a result of the dynamical bias. Since a similar decrease of the PVD was not found for optical galaxies, a systematic study is needed to quantify how the velocity statistics of different populations of galaxies are changed by the dynamical bias.

In this paper, we will use a cosmological hydrodynamic simulation to study the effect of spatial and dynamical biases on several velocity statistics of galaxies. Galaxies are identified in the simulation as clumps of cold and dense gas and classified into blue and red populations based on their formation epochs. We analyze the velocity statistics for different populations of galaxies as well as for dark matter. We not only measure the PVDs of the different tracers but also consider the mean infall velocity and the POTENT-style analysis. The latter two analyses have been used to measure the dynamical parameter $\beta = \Omega_0^{0.6}/b$ based on the (quasi-) linear perturbation theory of dark matter clustering

(Juszkiewicz et al. 2000; Dekel 1994; Nusser & Davis 1994). Since the observed velocity fields consist of the velocity data of spiral galaxies and/or elliptical galaxies, it is important to quantify whether the velocity statistics calculated based on various galaxy populations are biased relative to those of dark matter.

We separate the effects of the spatial and dynamical biases on these velocity statistics by constructing dynamically unbiased mock samples of galaxies and comparing their velocity statistics with those of galaxies in our simulation. One would expect that the dynamical friction mechanism operates in small dense regions, i.e., on small scales, but it is important to quantify on which scale the dynamical bias is significant for the statistics considered. The reason to separate the two biases is that the spatial bias is relatively easy to model for the velocity statistics if the occupation numbers of galaxies within halos are known or constrained from other observations (Mo, Jing, & Börner 1997; Jing et al. 1998; Seljak 2000; Peacock & Smith 2000; Sheth et al. 2001a, 2001b; Scoccimarro & Sheth 2002; Berlind & Weinberg 2002; Zheng et al. 2002; Kang et al. 2002; Kuwabara, Taruya, & Suto 2002; Yang, Mo, & van den Bosch 2003). We show quantitatively where the spatial bias models are applicable in interpreting the observations. In addition, in order to see the effect of dynamical friction on galaxies in a more direct manner, we also examine the motions of individual galaxies relative to their host dark halos and the relation between the velocity dispersion of member galaxies and that of dark matter in dark halos.

The rest of the paper is organized as follows. In § 2, we briefly describe our numerical simulation and our procedure to identify and classify galaxies. In § 3, some statistics for the velocity field of galaxies and dark matter are analyzed with emphasis on the effects of the spatial and dynamical biases. Finally, we summarize our findings in § 4.

2. SIMULATION

Our simulation is the same as that described in Yoshikawa et al. (2001), and details of the simulation can be found in Yoshikawa, Jing, & Suto (2000) and Yoshikawa et al. (2001). Here we briefly summarize some basic features.

The simulation code is a hybrid of a particle-particle-particle-mesh (P³M) Poisson solver and smoothed particle hydrodynamics (SPH). We adopt 128^3 dark matter particles and the same number of gas particles within a periodic simulation box of $L_{\text{box}} = 75 h^{-1} \text{ Mpc}$ per side. The cosmological model considered in this paper is a spatially flat low-density CDM universe with $\Omega_0 = 0.3$, $\lambda_0 = 0.7$, $\sigma_8 = 1.0$, and $h = 0.7$, where λ_0 is the dimensionless cosmological constant, σ_8 the rms density fluctuation at a scale of $8 h^{-1} \text{ Mpc}$, and h the Hubble parameter in units of $100 \text{ km s}^{-1} \text{ Mpc}^{-1}$. Furthermore, we set the baryonic density parameter to $\Omega_b = 0.015 h^{-2}$ (Copi, Schramm, & Turner 1995). Therefore, the masses of a single gas and dark matter particle are 2.4×10^9 and $2.2 \times 10^{10} M_\odot$, respectively. The ideal gas equation of state with an adiabatic index $\gamma = 5/3$ is adopted, and we consider the effect of radiative cooling, adopting the cooling rate with the metallicity $[\text{Fe}/\text{H}] = -0.5$ from Sutherland & Dopita (1993). In order to avoid numerical overcooling of gas particles in the SPH scheme, we implement the cold gas decoupling scheme, which was first introduced by Pearce

et al. (1999; see Yoshikawa et al. 2001 for a detailed implementation). The initial condition is created at redshift $z = 36$ and is evolved to $z = 0$.

We have 50 outputs at different redshifts between $z = 9$ and $z = 0$. For each output, galaxies are identified using the following procedure. First, we extract gas particles that satisfy the Jeans condition

$$h_{\text{SPH}} > \frac{c_s}{\sqrt{\pi G \rho}} \quad (1)$$

and the overdensity condition

$$\rho > 10^3 \bar{\rho}_b(z), \quad (2)$$

where h_{SPH} is the smoothing length of gas particles, c_s the sound speed, G the gravitational constant, ρ the SPH gas density, and $\bar{\rho}_b(z)$ the cosmic mean baryon density at redshift z . Then, we use the friends-of-friends (FOF) algorithm (Davis et al. 1985) to identify galaxies as clumps of these Jeans unstable gas particles. Here we adopt the FOF linking length of $b = 0.0164(1+z)\bar{l}$ as used in Yoshikawa et al. (2001), where \bar{l} is the mean separation of gas particles. We consider only galaxies with baryonic mass greater than $10^{11} M_\odot$, which is equivalent to 40 times the gas particle mass.

For each galaxy identified at $z = 0$, we define its formation redshift z_f as the epoch when one-half its member particles satisfy the conditions (1) and (2).

Using the formation redshift z_f of simulated galaxies, we classify those galaxies at $z = 0$ into two groups, the ones with $z_f < 1.8$ and the ones with $z_f > 1.8$, which we call, for later convenience, the “blue” and “red” galaxies, respectively. The value of threshold redshift $z_f = 1.8$ is chosen so that the blue and red populations have almost same number of galaxies just for the statistical significance of later analyses. In the procedures described above, we finally identify 1062 blue galaxies, 962 red galaxies, and 2024 galaxies in total at $z = 0$. Here it is not expected that such a simple categorization can explain the observed properties of early and late types of galaxies in any detail, but it can reproduce some statistical properties of observed galaxies qualitatively. Actually, as already discussed in Yoshikawa et al. (2001), the red galaxies reside within massive dark halos and the blue ones are preferentially formed in smaller dark halos. In addition, considering the observed correlation between galaxy types and their formation histories, blue and red galaxies in our simulation roughly correspond to late and early types of galaxies, respectively. Figure 1 shows the two-point correlation functions for red and blue galaxies. The profiles of the biasing parameter for each population of galaxies defined by

$$b_\xi(r) = \sqrt{\frac{\xi_{\text{gg}}(r)}{\xi(r)}} \quad (3)$$

are also shown in the lower panel, where $\xi_{\text{gg}}(r)$ and $\xi(r)$ are two-point correlation functions for galaxies and dark matter, respectively. The error bars indicate the 1σ Poisson error. We can see that the red galaxies exhibit a relatively higher amplitude of two-point correlation functions than the blue ones. This feature is consistent with the observed morphology-dependent clustering of galaxies (e.g., Loveday et al. 1995; Hermit et al. 1996; Norberg et al. 2002; Zehavi et al. 2002). We also plot the observed two-point correlation

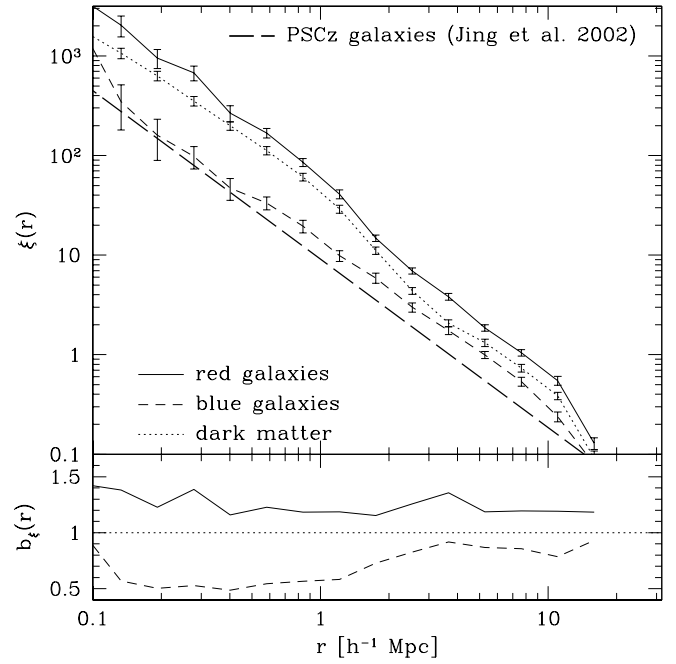


FIG. 1.—*Top*: Two-point correlation functions for blue galaxies, red galaxies, and dark matter. *Bottom*: Profiles of the bias parameter $b_\xi(r)$. For reference, we plot the two-point correlation function for the PSCz galaxies derived by Jing et al. (2002).

function of galaxies in the PSCz catalog,

$$\xi_{\text{PSCz}}(r) = \left(\frac{r}{3.7 \text{ h}^{-1} \text{ Mpc}} \right)^{-1.69}, \quad (4)$$

estimated by Jing et al. (2002). The two-point correlation function of the blue galaxies is relatively close to that of the PSCz galaxy sample compared with all and red galaxies. It is amazing to note that the $\xi(r)$ of the blue galaxies in our simulation is very close to the prediction of the cluster-weighted model of $\alpha = 0.25$ in Jing et al. (2002; see their Fig. 5). This spatial bias model with $\alpha = 0.25$ has been shown to be in good agreement with the projected two-point correlation function estimated from the PSCz catalog. This means that the blue galaxies in our simulation well represent the clustering properties of the galaxies in the PSCz catalog. Furthermore, since galaxies in the PSCz catalog are selected in the infrared waveband, they presumably have experienced star formation very recently or they are just undergoing star formation. Therefore, it is quite natural to consider that the blue galaxies in our simulation, which have been formed recently, indeed represent the physical properties of the PSCz galaxies.

3. VELOCITY STATISTICS

3.1. Pairwise Velocity Dispersion

Observationally, PVDs of galaxies can be measured by modeling the distortion of their two-point correlation function in redshift space. Therefore, observed PVDs are inevitably projected along the line of sight and functions of the projected separation. While, of course, three-dimensional PVDs obtained from the simulation cannot be directly compared with the observed ones, according to Jenkins et al.

(1998), we can calculate the projected line-of-sight PVD using three-dimensional PVD as

$$\sigma_{12}^2(r_p) = \frac{\int \xi(r) \sigma_{\text{proj}}^2(r) dl}{\int \xi(r) dl}, \quad (5)$$

where $\xi(r)$ is the two-point correlation function of objects we are considering and r_p and l denote the projected separation and the distance along the line of sight, respectively, and therefore $r^2 = r_p^2 + l^2$. The quantity σ_{proj}^2 is given by

$$\sigma_{\text{proj}}^2 = \frac{r_p^2 \sigma_v^2 + l^2 (\sigma_{\perp}^2 - v_{12}^2)}{r_p^2 + l^2}, \quad (6)$$

where σ_{\perp}^2 is the velocity dispersion perpendicular to the vector connecting each pair and v_{12} is the mean infall velocity described below.

Figure 2 shows the three-dimensional PVDs of dark matter and galaxies in our simulation. The quoted error bars indicate the 1σ Poisson error. As is shown in previous works (Jing et al. 1998; Benson et al. 2000), the PVD of all galaxies is markedly lower than that of the dark matter particles on all the scales considered. In Figure 2, we also show the PVDs of blue and red galaxies, separately. In Figure 3 we show the projected line-of-sight PVDs of dark matter, all galaxies, and blue and red galaxies. One can see that the PVD of the blue galaxies is much lower than that of the entire sample or of the red population, especially at small separation, down to $\sigma_v \sim 200 \text{ km s}^{-1}$ at $r = 0.1 h^{-1} \text{ Mpc}$ and $\sigma_{12} \sim 350 \text{ km s}^{-1}$ at $r_p = 0.1 h^{-1} \text{ Mpc}$. The PVD of the red galaxies is almost the same as or slightly higher than that of all galaxies. This behavior of the PVDs of the three populations of galaxies is qualitatively consistent with the PVD of galaxies in the LCRS (Jing et al. 1998), PSCz (Jing et al. 2002), and also SDSS data (Zehavi et al. 2002). In order to see the effect of selection of galaxies, in Figure 3, we also show the PVD of galaxies with higher mass

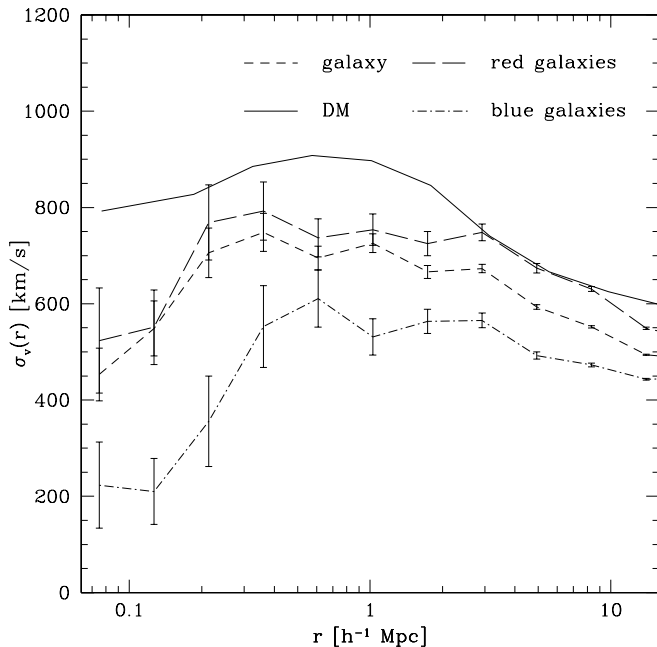


Fig. 2.—Three-dimensional pairwise velocity dispersions of dark matter particles, all galaxies, and red and blue galaxies.

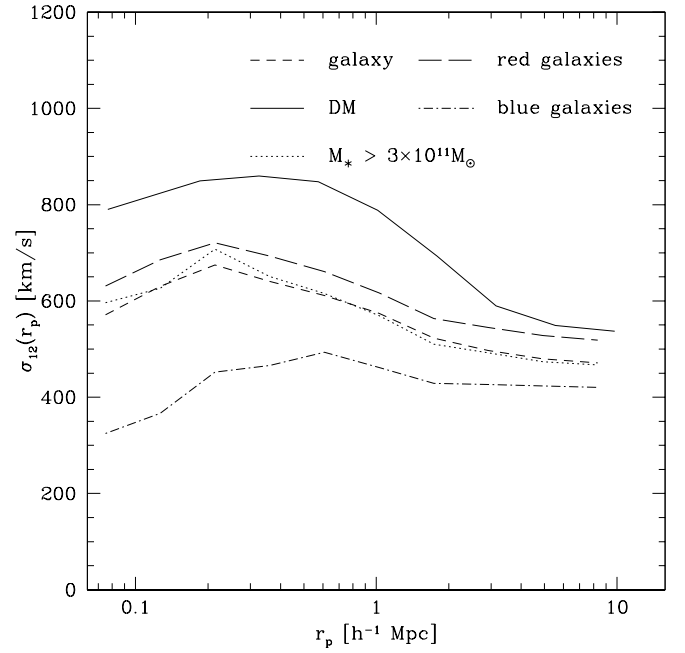


Fig. 3.—Same as Fig. 2 but for the PVDs projected along the line of sight.

$M_* > 3 \times 10^{11} M_{\odot}$. One can see that it is almost the same as the PVD of all galaxies and that our estimate of PVD is not sensitive to the selection of galaxies. The PVDs in the 2dFGRS (Hawkins et al. 2003) and the LCRS (Jing et al. 1998) are in good agreement with our result for large separation $r_p \gtrsim 0.5 h^{-1} \text{ Mpc}$, although our simulated PVD is slightly higher at $r_p < 0.5 h^{-1} \text{ Mpc}$. The difference at small separations can be partially ascribed to the effect of cosmic variance because PVD is generally quite sensitive to the presence and/or absence of rich galaxy clusters and because our simulation volume is smaller than the survey volumes of the 2dFGRS and the LCRS.

In order to discriminate between the effects of spatial and dynamical biases on the PVDs of galaxies, we create two types of mock galaxy samples from our simulation data. In the first sample, for each galaxy, we randomly select one *dark matter* particle within its host dark halo and assign to it the same formation redshift. The second sample is the same as the first one, except that the particles corresponding to the central massive galaxies in each halo are assigned the bulk motion velocity of the host halo; i.e., these particles are static in their host dark halos. Therefore, these samples mimic the spatial distribution of galaxies but keep the properties of the dark matter velocity field and can be regarded as spatially biased and dynamically unbiased samples. For later convenience, we call the first and second dynamically unbiased samples DU-I and DU-II, respectively. We construct 20 realizations of these dynamically unbiased samples of all galaxies and of the blue galaxies by selecting particles with the assigned formation redshift less than 1.8. We confirm that the two-point correlation functions of these samples agree well with those of corresponding galaxy samples. In Figure 4, we show the three-dimensional PVDs of the DU-I and DU-II samples for all the galaxies as well as for the blue galaxies. The error bars indicate the statistical dispersion for 20 realizations of the samples. One can see that the PVD of all galaxies (*solid line in the lower panel*) is in

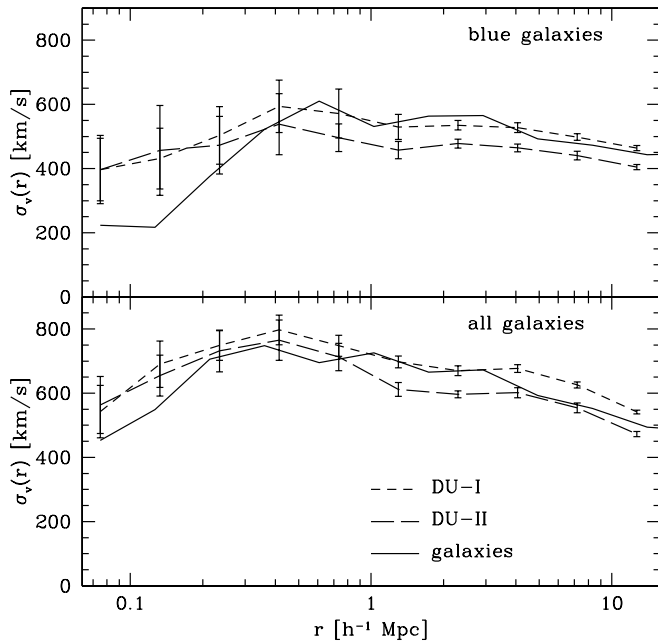


FIG. 4.—Pairwise velocity dispersions of the two dynamically unbiased samples and galaxies for the whole population (*top*) and the blue population (*bottom*).

reasonable agreement with the DU-I and DU-II samples. This indicates that the lower PVDs of all the galaxies can be explained by the different spatial distribution between galaxies and dark matter. This result is consistent with previous work (Jing et al. 1998; Benson et al. 2000), and we confirm it more directly by comparing the galaxy sample and the dynamically unbiased samples. On the other hand, the PVD of the blue galaxies (*solid line in the upper panel*) deviates downward from that of the DU-I and DU-II samples at the

small separation of $r < 0.3 h^{-1}$ Mpc; therefore, it cannot be explained only by the spatial bias. Figure 5 shows that the line-of-sight projected PVDs exhibit the same results as in the case of the three-dimensional PVDs. We can suggest that the rapid decrease of the PVD of late-type galaxies found in the PSCz catalog (Jing et al. 2002) and SDSS galaxies (Zehavi et al. 2002) is due to the effect of dynamical friction. More evidence is given in § 3.4.

Let us note the comparison with the previous works by Benson et al. (2000) and Kauffmann et al. (1999). First, it should be noted that in these two works, “galaxies” are formed according to a combination of dissipationless N -body simulations and semianalytic galaxy formation schemes, while the “galaxies” in our SPH simulation are identified as clumps of cold and dense gas particles. Kauffmann et al. (1999) found very similar PVDs for galaxies and dark matter, which are not consistent with recent observational results (Jing et al. 1998, 2002; Zehavi et al. 2002) and Benson et al. (2000). Actually, the line-of-sight projected PVD of all galaxies in our simulation also significantly departs from that of dark matter and is consistent with the result of Benson et al. (2000). Benson et al. (2000) argued that the discrepancy with Kauffmann et al. (1999) is due to the different frequency with which dark halos are populated with a particular number of galaxies in their semianalytic schemes. Since our galaxies are identified in a totally different manner from Benson et al. (2000) and Kauffmann et al. (1999) as described above, our result gives independent verification for the result of Benson et al. (2000). In Benson et al. (2000), since the galaxies’ positions and velocities are assigned those of dark matter particles that are randomly chosen within host dark matter halos, except for central galaxies of dark halos, which are assigned the positions and velocities of mass centers of their host dark halos, their galaxy sample is, by construction, free from the dynamical friction, and somewhat similar to our DU-II sample. Therefore, their estimation of galaxies’ PVD missed the effect of dynamical bias, which we focus on throughout in this paper.

3.2. Mean Infall Velocity

The mean infall velocity $v_{12}(r)$ of galaxies can be also used to constrain the cosmological density parameters Ω_0 (Juszkiewicz et al. 2000), according to a simple analytic expression for v_{12} of the dark matter by Juszkiewicz, Springel, & Durrer (1999) as

$$v_{12}(r) = -\frac{2}{3} H r \Omega_0^{0.6} \bar{\xi}(r) [1 + \alpha \bar{\xi}(r)] , \quad (7)$$

$$\bar{\xi}(r) = \frac{3}{r^3 [1 + \xi(r)]} \int_0^r \xi(x) x^2 dx , \quad (8)$$

where $\alpha = 1.2 - 0.65\gamma$, $\gamma = -(d \ln \xi / d \ln r)_{\xi=1}$, and H is the Hubble constant. It should be pointed out that in order to use equation (7) to measure β , the galaxies used must trace the underlying dark matter in the spatial and in the velocity distributions. Figure 6 shows $v_{12}(r)$ for dark matter, all galaxies, and blue and red galaxy samples in our simulation. Apparently, the blue galaxies have a significantly smaller infall velocity $v_{12}(r)$ than the red galaxies or all galaxies at all separations considered. This is not consistent with the result of Juszkiewicz et al. (2000), in which they conclude that there is no difference in v_{12} between early and late-type galaxies. This is probably because their estimation of $v_{12}(r)$

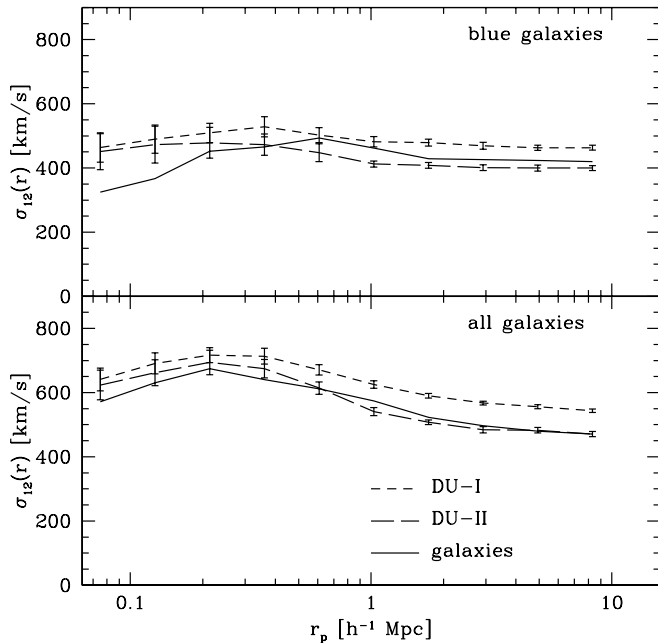


FIG. 5.—Same as Fig. 4 but for the PVDs projected along the line of sight.

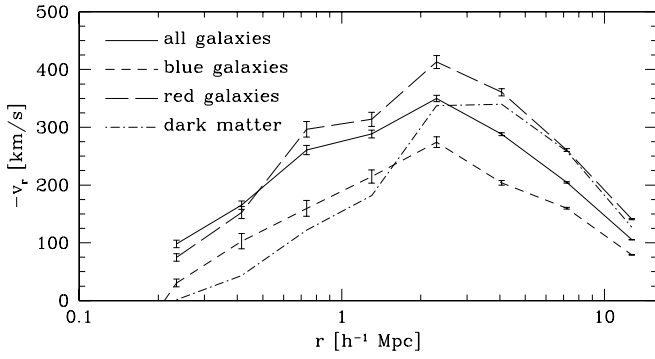


FIG. 6.—Mean infall velocity of dark matter, all galaxies, blue galaxies, and red galaxies.

for elliptical galaxies has large observational uncertainties. Actually, the number of elliptical galaxies used in Juszkiewicz et al. (2000) is not sufficient for the definite estimation of the mean infall velocity. In Figure 7, the mean infall velocity for the DU-I and DU-II samples of all and of blue galaxies are depicted. The error bars indicate the statistical dispersion for 20 realizations of the DU-I and DU-II samples. At large separations with $r \gtrsim 2 h^{-1}$ Mpc, the mean infall velocities of the galaxies are well reproduced by the corresponding DU-I and DU-II samples. Thus, the difference in $v_{12}(r)$ for all and for blue galaxies is mostly due to the difference in the spatial distributions. As is done in Juszkiewicz et al. (2000), one can determine the values of Ω_0 and σ_8 from the value of $v_{12}(r)$ at a certain separation, say, $r = 10 h^{-1}$ Mpc, using equation (7), if the spatial bias of the observed $v_{12}(r)$ is properly corrected. However, if one simply adopts the mean infall velocity of all the galaxies or the blue ones, which is lower than that of dark matter, the estimated Ω_0 can be underestimated for a given value of σ_8 and vice versa (cf. Juszkiewicz et al. 2000).

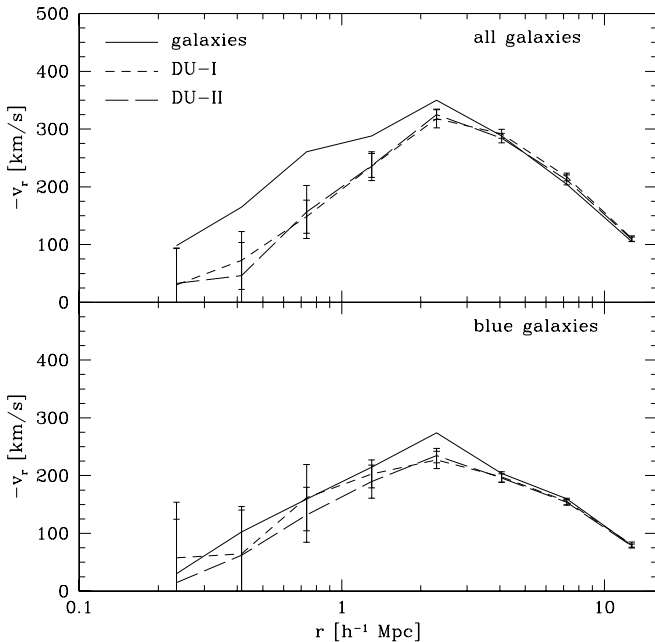


FIG. 7.—Mean infall velocity of the DU-I and DU-II mock samples of the whole sample, and of the blue galaxies. The results from the full simulation for all galaxies and for blue galaxies are shown for comparison.

3.3. Mass Reconstruction Analysis

In this subsection, we calculate the mass density field reconstructed using a method similar to the POTENT analysis (see Dekel 1994; Dekel et al. 1999 for review) in order to investigate how the spatial and dynamical biases on galaxies can affect the results of the POTENT analysis. In practice, the POTENT analysis attempts to recover the mass density field from a catalog of radial velocities of galaxies using the assumption that the galaxy velocity field is irrotational, $\nabla \times \mathbf{v} = 0$, and it involves a slightly complicated statistical treatment of observational data. In this paper, however, since we are purely interested in the effect of spatial and dynamical biases, we reconstruct mass density fields from three-dimensional velocity data. Specifically, in order to recover the mass density fields, we use the following quasi-linear approximation of the continuity equation (Dekel et al. 1999):

$$\delta_{\text{POT}} = -(1 + \epsilon_1)f^{-1}\nabla \cdot \mathbf{v} - (1 + \epsilon_2)f^{-2}\Delta_2 + (1 + \epsilon_3)f^{-3}\Delta_3, \quad (9)$$

where

$$\Delta_2 = \sum_{i < j} \left[\left(\frac{\partial v_i}{\partial x_j} \right)^2 - \frac{\partial v_i}{\partial x_i} \frac{\partial v_j}{\partial x_j} \right] \quad (10)$$

and

$$\Delta_3 = \sum_{i,j,k} \left(\frac{\partial v_i}{\partial x_i} \frac{\partial v_j}{\partial x_k} \frac{\partial v_k}{\partial x_j} - \frac{\partial v_i}{\partial x_i} \frac{\partial v_j}{\partial x_j} \frac{\partial v_k}{\partial x_k} \right). \quad (11)$$

In equation (11), the sum is over three cyclic permutations of $(i, j, k) = (1, 2, 3)$. The three parameters ϵ_1 , ϵ_2 , and ϵ_3 are empirically tuned to best fit the dark matter density field, and we adopt $\epsilon_1 = 0.06$, $\epsilon_2 = -0.13$, and $\epsilon_3 = -0.3$ throughout this paper.

In the analysis, we calculate the mass and galaxy density fields using the cloud-in-cell (CIC) scheme. We also compute a volume-weighted velocity field of galaxies with a smoothing scale R_s according to the following steps (Babul et al. 1994; Berlind, Narayanan, & Weinberg 2001). First, we create the momentum field of galaxies using CIC binning and smooth it with a Gaussian filter of a smoothing scale R_1 , where R_1 must be much smaller than the smoothing scale R_s . Second, we divide the smoothed momentum field by a similarly smoothed density field of galaxies. Note that this is a mass-weighted velocity field smoothed over the scale R_1 . Finally, we smooth this velocity field with another Gaussian filter of smoothing scale $R_2 = (R_s^2 - R_1^2)^{1/2}$ to form the volume-weighted velocity field smoothed with the effective smoothing scale of R_s . In our analysis, we adopt $R_1 = 1 h^{-1}$ Mpc and we calculate the reconstructed density field δ_{POT} for $R_s = 8$ and $12 h^{-1}$ Mpc according to equation (9). The smoothing scale adopted in the actual POTENT analyses is typically $R_s = 10$ – $12 h^{-1}$ Mpc in order to minimize the effect of inhomogeneous Malmquist bias. In this paper, however, we are interested in the effects of the spatial and dynamical biases on the POTENT method, and apply it for a slightly smaller smoothing scale $R_s = 8 h^{-1}$ Mpc.

Figures 8 and 9 show the joint probability distributions of δ_m and δ_{POT} reconstructed from the velocity fields of dark matter, all galaxies, and blue galaxies (Figs. 8 and 9, lower panels) for $R_s = 12$ and $8 h^{-1}$ Mpc, respectively. The gray

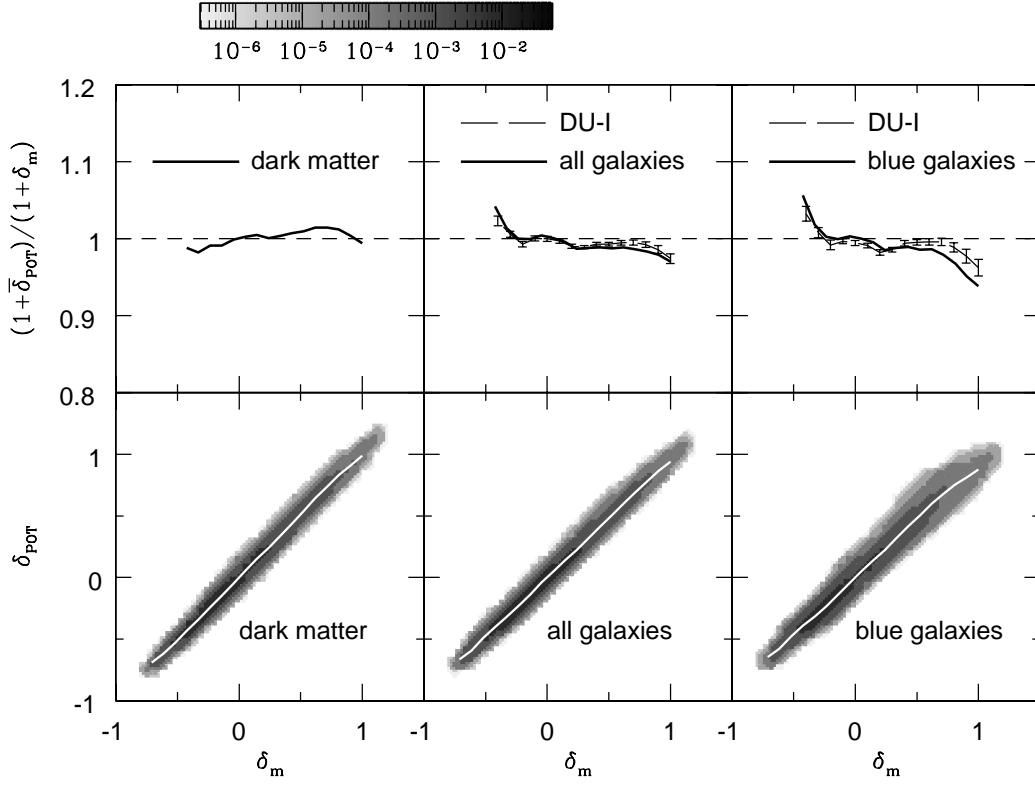


FIG. 8.—*Bottom:* Joint probability distributions of the mass density field δ_m and that reconstructed using the POTENT-style method δ_{POT} . The gray scale indicates the joint probability that a region has a set of values δ_m and δ_{POT} , simultaneously. The solid lines indicate the mean relation $\bar{\delta}_{\text{POT}}(\delta_m)$ between δ_m and δ_{POT} . The smoothing scale is set to $R_s = 12 h^{-1}$ Mpc. *Top:* Ratio of $(1 + \bar{\delta}_{\text{POT}})$ to $(1 + \delta_m)$ as a function of δ_m . We also show the ratio calculated from the DU-I sample in long-dashed lines.

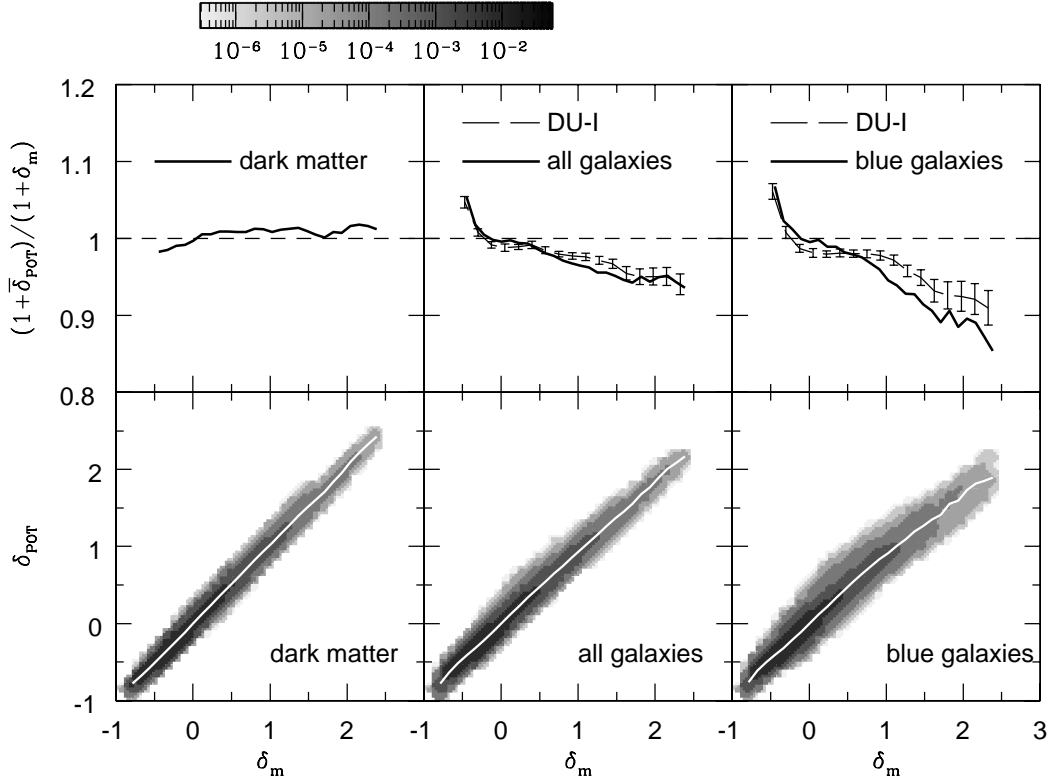


FIG. 9.—Same as Fig. 8 but for $R_s = 8 h^{-1}$ Mpc

scale indicates the joint probability that a region has a set of the actual mass overdensity δ_m and the reconstructed one δ_{POT} , simultaneously. We also show the ratio of $(1 + \delta_{\text{POT}})$ relative to $(1 + \delta_m)$ in solid lines (Figs. 8 and 9, *upper panels*), where δ_{POT} is the mean of δ_{POT} for a given δ_m . For smoothing scales of both $R_s = 8$ and $12 h^{-1}$ Mpc, the dark matter velocity fields well reproduce the real density field with good accuracy. This indicates that the adopted reconstruction method provides correct density estimation if a spatially and dynamically unbiased sample of particles is given. This also confirms that equation (9) works well for the quasi-linear regions (Dekel et al. 1999). In the case of $R_s = 12 h^{-1}$ Mpc, the reconstructed density fields agree well with the real ones for $\delta_m \gtrsim 0$ irrespective of the adopted tracers, while δ_{POT} reconstructed from the velocity of the blue galaxies is slightly underestimated by $\simeq 5\%$ at high-density ($\delta_m \simeq 1$) regions. On the other hand, for $R_s = 8 h^{-1}$ Mpc, the reconstructed density fields from the velocity fields of the blue galaxies and all galaxies are systematically underestimated at high-density regions by $\sim 15\%$ and $\sim 5\%$, respectively.

In order to estimate to what extent the effects of dynamical friction and spatial bias are important for the discrepancy between δ_m and δ_{POT} , we carry out the POTENT-style density reconstruction for the DU-I and DU-II samples of all and of blue galaxies and compare the results with those of galaxy samples. In the upper panels of Figures 8 and 9, long-dashed lines with error bars show the ratio of $(1 + \delta_{\text{POT}})$ and $(1 + \delta_m)$ reconstructed from the velocity fields of the DU-I sample. We omit the results from the DU-II sample since they are almost identical to the DU-I sample. The error bars indicate the statistical dispersion for 20 realizations of the DU-I samples. In the case of $R_s = 12 h^{-1}$ Mpc, which is usually adopted in recent POTENT analyses, we can see that the POTENT-style analyses are not seriously affected by the spatial and dynamical biases, although the dynamical bias is only slightly effective at the high-density regions for blue galaxies. In adopting the smoothing scale $R_s = 8 h^{-1}$ Mpc, we have no significant difference between δ_{POT} recovered from the DU-I sample and from all the galaxies, indicating that the dynamical bias is not important for all galaxies and that only the spatial bias is responsible for the discrepancy. On the other hand, as for the blue galaxy samples, although the density field reconstructed from the DU-I sample of blue galaxies underestimates the real one, the one reconstructed from the velocity of the blue galaxies is still lower than that of the DU-I sample. This indicates that the dynamical bias is not negligible for blue galaxies on this smoothing scale.

As for the spatial bias, as is shown in Yoshikawa et al. (2001), blue galaxies in our simulation are antibiased in high-density regions. Thus, the velocity field calculated from the blue galaxies is inhomogeneously sampled and does not faithfully represent the underlying dark matter velocity, especially at high mass density regions and for smaller smoothing scales. In our analyses, in the case of $R_s = 8 h^{-1}$ Mpc, as shown in Figure 9, the effect of the spatial bias leads to an underestimate of the real density field by $\simeq 10\%$. Actually, much work has been done to understand and control this problem (Dekel et al. 1999). Other reconstruction methods and some algorithms to estimate the β -parameter from velocity data of galaxies have been proposed (Zaroubi et al. 1995; Willick et al. 1997; Zaroubi, Hoffman, & Dekel 1999) that prevent the effect of the spatial

bias to some extent. However, these methods still cannot escape from the dynamical bias because it is implicitly assumed that there is no dynamical bias in the observed velocity field. Therefore, when the velocity data of late-type galaxies smoothed over the scale of $R_s = 8 h^{-1}$ Mpc or smaller are adopted, the reconstructed density field and the estimated β -value can be skewed because of the dynamical bias.

3.4. Motion of Galaxies within Dark Halos

Thus far, we have shown the velocity statistics of galaxies in a cosmological volume. In this subsection, we focus on the statistics of motion of galaxies relative to their host dark halos. Figure 10 shows the distributions of velocities of the three most massive galaxies in each dark halo relative to the average velocity (i.e., the velocity of the mass center) of the host dark halo. Here we normalized the velocity of the galaxies by the three-dimensional velocity dispersion of the dark matter inside the dark halos. The most massive galaxy in each dark halo is almost static within the host dark halo, consistent with the observation of cD galaxies in galaxy clusters (Oegerle & Hill 2001). The distributions of the second- and third-ranked galaxies are skewed toward the smaller velocities because they should have a peak at $v_{\text{gal}}/\sigma_{\text{halo}}^{3d} \simeq 1$ if the motion of the galaxies is the same as that of the dark matter, free from velocity bias. Furthermore, the ratio of the velocity dispersions of galaxies σ_{gal} and dark matter σ_{dm} inside each dark halo is plotted in Figure 11. Representative error bars for halos of different mass are indicated in the figure that are the standard scatters of the dispersion ratio at that halo mass. Velocity dispersions of galaxies in relatively low mass ($\simeq 10^{13} M_\odot$) dark halos are systematically smaller than those of dark matter, while for a very massive dark halo with mass greater than $10^{14} M_\odot$, we have $\sigma_{\text{gal}} \simeq \sigma_{\text{dm}}$. This result is due to the fact that the central

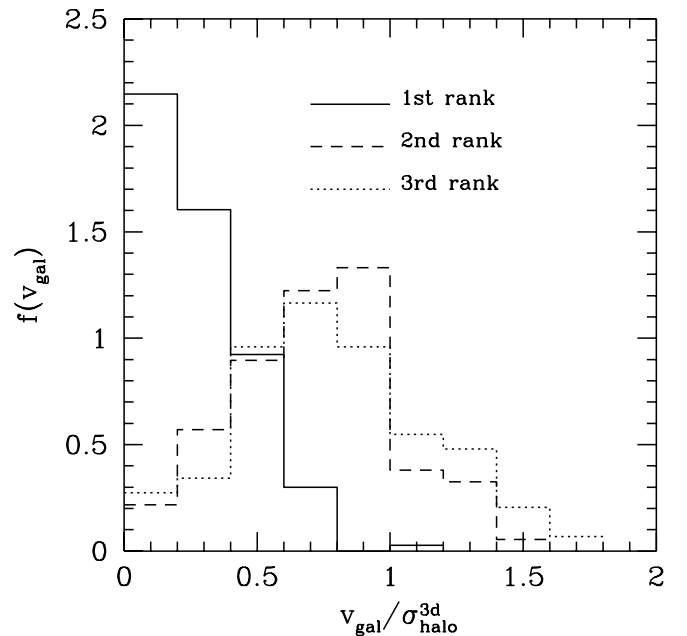


FIG. 10.—Distributions of relative velocity of the three most massive galaxies to each host dark halo. The velocity of galaxies is scaled by the three-dimensional velocity dispersion of the dark matter particles inside their host halos.

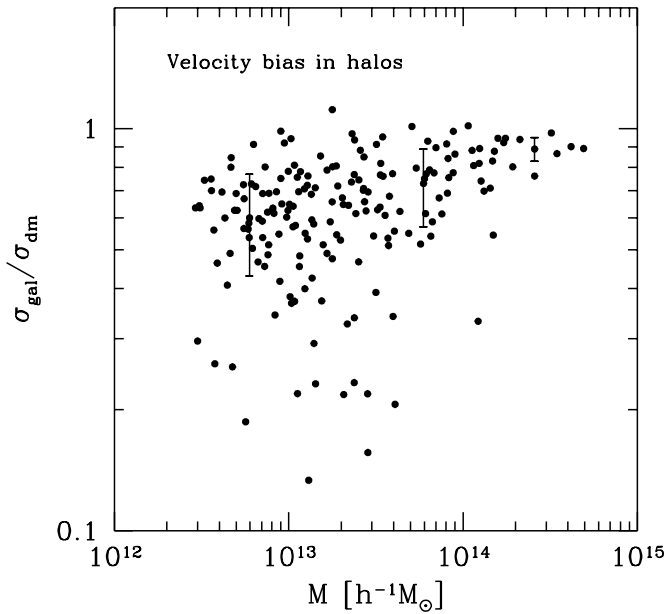


FIG. 11.—Ratio of the velocity dispersion of galaxies to that of dark matter in each dark halo as a function of halo mass. Representative error bars for individual halos of different mass are also indicated.

galaxies are static, and the other galaxies are slowed down, significantly especially in small halos, by dynamical friction. This result also shows why the PVDs of blue galaxies are small, because the blue galaxies mainly reside in smaller dark halos, and the PVDs at small separation have their main contribution from pairs of galaxies within the same dark halo. If we use a larger mass cut for defining galaxies, we expect the dispersion ratio will systematically decrease because the dynamical friction bias is more effective for more massive objects (see § 4 for further discussion).

From these two statistics, we find that in each dark halo the motion of galaxies is affected by dynamical friction, and their velocity is less than that of dark matter. Since the blue galaxies in our simulation statistically tend to be less massive and preferentially reside in smaller dark halos, these results indicate that the blue galaxies are selectively affected by dynamical friction. Furthermore, the implication for the velocity dispersion of galaxies, which has been conventionally used to estimate the mass of clusters and groups of galaxies (Bahcall & Tremaine 1981; Zabludoff et al. 1993; Wu & Fang 1997; Girardi & Giuricin 2000; Girardi et al. 2002), is that the mass of groups of galaxies based on the velocity dispersion of galaxies could be seriously underestimated.

4. SUMMARY AND DISCUSSION

In this paper, we have investigated several velocity statistics of galaxies and their biases relative to dark matter particles using cosmological hydrodynamic simulations. We consider the PVD, the mean infall velocity, and the POTENT-style analysis for all galaxies identified in our simulation and for two subsamples, the blue and red galaxies, categorized based on their formation epochs. We also construct dynamically unbiased samples of all and of blue galaxies, which mimic the spatial distributions of galaxies but still keep the same dynamical properties as the dark matter, and measure their velocity statistics in order to investigate

the effects of the spatial and dynamical biases of galaxies on their velocity statistics.

Our major findings are as follows.

1. The PVD of all galaxies is systematically lower than that of the dark matter, and the blue galaxies have a lower PVD than galaxies from the whole sample, especially at small separation. This is consistent with previous observational results (Jing et al. 1998, 2002; Zehavi et al. 2002). According to our analyses, the low PVD of all the galaxies is due mostly to the difference of the spatial distributions between galaxies and dark matter. On the other hand, the discrepancy in the PVD between dark matter and the blue galaxies cannot be explained only by the spatial bias, and it is suggested that there must be an effect of the dynamical bias for the blue galaxies.

2. The mean infall velocity of the blue galaxies is significantly lower than that of the whole sample and of the red galaxies. The dark matter particles show almost the same values as the red galaxies at $r \gtrsim 3 h^{-1} \text{ Mpc}$ and $\simeq 100 \text{ km s}^{-1}$ lower than the whole sample and the red galaxies at $r \lesssim 1 h^{-1} \text{ Mpc}$. In estimating Ω_0 and σ_8 from the mean infall velocity of all the galaxies or of the late-type galaxies at the separation of $r = 10 h^{-1} \text{ Mpc}$, one will underestimate Ω_0 for a given value of σ_8 and vice versa. We also find that the difference at the separation $r \gtrsim 3 h^{-1} \text{ Mpc}$ is due only to the difference in the spatial distribution among galaxy populations.

3. Our analysis shows that the POTENT-style mass density reconstruction using galaxies' peculiar velocity is almost free from the spatial and dynamical biases on the smoothing scale of $R_s = 12 h^{-1} \text{ Mpc}$, which is typically adopted in recent POTENT analyses. On the other hand, in the case of $R_s = 8 h^{-1} \text{ Mpc}$, it suffers from spatial bias if the velocity data of all galaxies are adopted, and furthermore, the dynamical bias is also important when we use the velocity field of the blue galaxies. Some methods to probe the β -parameter based on velocity-velocity comparisons (Davis, Nusser, & Willick 1996; Willick et al. 1997) and the mass density reconstruction based on the Wiener filtering (Zaroubi et al. 1995, 1999) can evade the effect of the spatial bias to some extent and probe the mass density or velocity on smaller scales, but they can still suffer from the dynamical bias on smoothing scales equal to or smaller than $R_s = 8 h^{-1} \text{ Mpc}$ if the velocity data of late-type galaxies are adopted.

4. In each dark halo, the most massive galaxy is almost static within the dark halo. The velocity of the second- and third-ranking massive galaxies relative to their host dark halos is statistically smaller than that of the dark matter inside the halos because of dynamical friction. Furthermore, the velocity dispersions of galaxies in less massive ($\sim 10^{13} M_{\odot}$) dark halos are systematically lower than those of dark matter particles inside dark halos. This bias in the velocity dispersion of the galaxies leads to serious underestimates of the mass of groups of galaxies. It is also responsible for the low PVD value of the blue galaxies.

The reason why the blue galaxies are selectively affected by dynamical friction is tightly related to their formation epochs and can be qualitatively explained as follows. According to the standard scenario of galaxy formation, galaxies form in the gravitational potential wells provided by the dark matter halos and dark matter clumps inside dark halos. The red galaxies are formed within more

massive halos than the blue ones, and they experience a significant number of merging processes. The mergers mix gas and dark matter and thus reduce the differences in the distribution. The blue galaxies form in less massive halos and have fewer mergers during their formation history. Their mass is a bigger fraction of the host halo mass, and thus they are efficiently slowed down relative to the center of mass of the halo by dynamical friction.

Our definition of galaxies in our simulation data is admittedly rather phenomenological. A more observationally oriented classification of galaxies, for example, using color or magnitude of galaxies, is needed for a direct comparison with observations. We plan to implement more realistic prescriptions of galaxy formation and evolution including star formation, feedback, and UV background heating in due course. However, it is encouraging that even

these simple prescription of galaxy formation can reproduce the clustering and the PVDs of the observed galaxies. Thus, we believe that the results presented in this paper are quite robust and that it is worth considering the importance of dynamical friction for the velocity statistics of galaxies.

We thank Yasushi Suto and Takashi Hamana for several enlightening discussions and an anonymous referee for suggesting some improvements in this manuscript. Numerical simulations presented in this paper were carried out at ADAC (the Astronomical Data Analysis Center) of the National Astronomical Observatory, Japan, and at KEK (High Energy Accelerator Research Organization, Japan). Y. P. J. was supported in part by NKBRF (G19990754) and by NSFC (10125314).

REFERENCES

- Babul, A., Weinberg, D. H., Dekel, A., & Ostriker, J. P. 1994, *ApJ*, 427, 1
Bahcall, N. A., & Comerford, J. M. 2002, *ApJ*, 565, L5
Bahcall, N. A., & Tremaine, S. 1981, *ApJ*, 244, 805
Benson, A. J., Baugh, C. M., Cole, S., Frenk, C. S., & Lacey, C. G. 2000, *MNRAS*, 316, 107
Berlind, A. A., Narayanan, V. K., & Weinberg, D. H. 2001, *ApJ*, 549, 688
Berlind, A. A., & Weinberg, D. H. 2002, *ApJ*, 575, 587
Bertschinger, E., & Dekel, A. 1989, *ApJ*, 336, L5
Carlberg, R. G., Yee, H. K. C., Ellingson, E., Abraham, R., Gravel, P., Morris, S., & Pritchet, C. J. 1996, *ApJ*, 462, 32
Cen, R., & Ostriker, J. P. 2000, *ApJ*, 538, 83
Copi, C. J., Schramm, D. N., & Turner, M. S. 1995, *ApJ*, 455, L95
Davis, M., Efstathiou, G., Frenk, C. S., & White, S. D. M. 1985, *ApJ*, 292, 371
Davis, M., Nusser, A., & Willick, J. A. 1996, *ApJ*, 473, 22
Davis, M., & Peebles, P. J. E. 1983, *ApJ*, 267, 465
Dekel, A. 1994, *ARA&A*, 32, 371
Dekel, A., Eldar, A., Kolatt, T., Yahil, A., Willick, J. A., Faber, S. M., Courteau, S., & Burstein, D. 1999, *ApJ*, 522, 1
Fisher, K. B., Davis, M., Strauss, M. A., Yahil, A., & Huchra, J. P. 1994, *MNRAS*, 266, 50
Frenk, C. S., Evrard, A. E., White, S. D. M., & Summers, F. J. 1996, *ApJ*, 472, 460
Girardi, M., & Giuricin, G. 2000, *ApJ*, 540, 45
Girardi, M., Manzato, P., Mezzetti, M., Giuricin, G., & Limboz, F. 2002, *ApJ*, 569, 720
Hawkins, E., et al. 2003, *MNRAS*, submitted (astro-ph/0212375)
Hermit, S., Santiago, B. X., Lahav, O., Strauss, M. A., Davis, M., Dressler, A., & Huchra, J. P. 1996, *MNRAS*, 283, 709
Jenkins, A., et al. 1998, *ApJ*, 499, 20
Jing, Y. P., Börner, G., & Suto, Y. 2002, *ApJ*, 564, 15 (JBS02)
Jing, Y. P., Mo, H. J., & Börner, G. 1998, *ApJ*, 494, 1
Juszkiewicz, R., Ferreira, P. G., Feldman, H. A., Jaffe, A. H., & Davis, M. 2000, *Science*, 287, 109
Juszkiewicz, R., Springel, V., & Durrer, R. 1999, *ApJ*, 518, L25
Kang, X., Jing, Y. P., Mo, H. J., & Börner, G. 2002, *MNRAS*, 336, 892
Katz, N., Hernquist, L., & Weinberg, D. H. 1992, *ApJ*, 399, L109
Kauffmann, G., Colberg, J. M., Diaferio, A., & White, S. D. M. 1999, *MNRAS*, 303, 188
Kuwabara, T., Taruya, A., & Suto, Y. 2002, *PASJ*, 54, 503
Loveday, J., Maddox, S. J., Efstathiou, G., & Peterson, B. A. 1995, *ApJ*, 442, 457
Mo, H. J., Jing, Y. P., & Börner, G. 1993, *MNRAS*, 264, 825
———. 1997, *MNRAS*, 286, 979
Norberg, P., et al. 2002, *MNRAS*, 332, 827
Nusser, A., & Davis, M. 1994, *ApJ*, 421, L1
Oegerle, W. R., & Hill, J. M. 2001, *AJ*, 122, 2858
Ostriker, J. P., & Suto, Y. 1990, *ApJ*, 348, 378
Peacock, J. A., & Smith, R. E. 2000, *MNRAS*, 318, 1144
Peacock, J. A., et al. 2001, *Nature*, 410, 169
Pearce, F. R., Jenkins, A., Frenk, C. S., White, S. D. M., Thomas, P. A., Couchman, H. M. P., Peacock, J. A., & Efstathiou, G. 2001, *MNRAS*, 326, 649
Pearce, F. R., et al. 1999, *ApJ*, 521, L99
Saunders, W., et al. 2000, *MNRAS*, 317, 55
Scoccimarro, R., & Sheth, R. K. 2002, *MNRAS*, 329, 629
Seljak, U. 2000, *MNRAS*, 318, 203
Shectman, S. A., Landy, S. D., Oemler, A., Tucker, D. L., Lin, H., Kirshner, R. P., & Schechter, P. L. 1996, *ApJ*, 470, 172
Sheth, R. K., Diaferio, A., Hui, L., & Scoccimarro, R. 2001a, *MNRAS*, 326, 463
Sheth, R. K., Hui, L., Diaferio, A., & Scoccimarro, R. 2001b, *MNRAS*, 325, 1288
Sigad, Y., Eldar, A., Dekel, A., Strauss, M., & Yahil, A. 1998, *ApJ*, 495, 516
Sutherland, R. S., & Dopita, M. A. 1993, *ApJS*, 88, 253
Suto, Y. 1993, *Prog. Theor. Phys.*, 90, 1173
Suto, Y., & Jing, Y. P. 1997, *ApJS*, 110, 167
Willick, J. A., Strauss, M. A., Dekel, A., & Kollat, T. 1997, *ApJ*, 486, 629
Wu, X., & Fang, L. 1997, *ApJ*, 483, 62
Yang, X. H., Mo, H. J., & van den Bosch, F. C. 2003, *MNRAS*, 339, 1057
Yoshikawa, K., Jing, Y. P., & Suto, Y. 2000, *ApJ*, 535, 593
Yoshikawa, K., Taruya, A., Jing, Y. P., & Suto, Y. 2001, *ApJ*, 558, 520
Zabludoff, A. I., Geller, M. J., Huchra, J. P., & Ramella, M. 1993, *AJ*, 106, 1301
Zaroubi, S. 2002, *MNRAS*, 331, 901
Zaroubi, S., Hoffman, Y., & Dekel, A. 1999, *ApJ*, 520, 413
Zaroubi, S., Hoffman, Y., Fisher, K. B., & Lahav, O. 1995, *ApJ*, 449, 446
Zehavi, I., et al. 2002, *ApJ*, 571, 172
Zheng, Z., Tinker, J. L., Weinberg, D. H., & Berlind, A. A. 2002, *ApJ*, 575, 617